Chemical Engineering Journal 166 (2011) 744–750

Contents lists available at ScienceDirect

Chemical Engineering Journal

journal homepage: www.elsevier.com/locate/cej

Microwave preparation of Ti-containing mesoporous materials. Application as catalysts for transesterification

Yun Shi, Shengping Wang*, Xinbin Ma**

Key Laboratory for Green Chemical Technology of Ministry of Education, School of Chemical Engineering and Technology, Tianjin University, Tianjin 300072, China

ARTICLE INFO

Article history:
Received 20 July 2010
Received in revised form
10 November 2010
Accepted 22 November 2010

Keywords:
Titanium
Mesoporous materials
Microwave irradiation
Transesterification
Diphenyl oxalate

ABSTRACT

Titanium-containing mesoporous (Ti-MCM-41) materials were prepared by microwave irradiation method at different temperature (from 353 K to 413 K) in 40 min, a much shorter period of crystallization time than that by hydrothermal method. Various characterization techniques, including XRD, FT-IR, N_2 adsorption and desorption, ICP, DRUV–vis, pyridine-FTIR, NH_3-TPD and particle size analysis were carried out to investigate the physicochemical properties of these samples. Results showed that the samples prepared by microwave irradiation method have typical long-range order of hexagonal MCM-41 structure. Titanium incorporates into the silica framework and Ti species are mostly in tetrahedral coordination. Ti-MCM-41 molecular sieves were active as catalysts for transesterification of dimethyl oxalate and phenol to produce diphenyl oxalate and the optimal heating temperature is 393 K. The small particle size, large surface area and plenty of Ti(IV) active centers inside the framework, which provide more weak acid sites, are favorable for improving the catalytic properties.

1. Introduction

As a member of M41S family, MCM-41 mesoporous molecular sieve, with a hexagonal arrangement of mono-dimensional pores, has drawn widely attention since its invention in 1992 [1]. Owing to their exceptional adsorption capacities and molecular sieving properties, these mesoporous materials have many potential applications in the pharmaceutical and fine chemical industries, petroleum refining, adsorption and separation processes and heterocatalysis. However, the catalytic properties of MCM-41 molecular sieve are poor because of the lacking of active sites in the neutral purely siliceous framework, which limits its application as heterogeneous catalysts. As reported [2,3], the incorporation of heteroatoms as extra-framework nanoscale oxide clusters or in their appropriate valence state as tetrahedral framework species may generate active sites. In particular, mesoporous silicate materials containing titanium are very attractive for its good acid and redox properties. Therefore, a lot of studies were carried out for the synthesis of Ti-MCM-41 catalysts. Corma and coworkers [4] utilized a classical hydrothermal method with cationic surfactants template; Galacho et al. [5] prepared high Ti content mesoporous molecular sieves at room temperature; Guidotti et al. [6] used titanocene dichloride as titanium precursor following a grafting methodology; Wu et al. [7] designed a solid–gas reaction between siliceous MCM-41 and $TiCl_3$ vapor for Ti-MCM-41 synthesis, etc. The most commonly applied method was hydrothermally synthesis [4,8–10] in the previously reported literatures. At present, microwave irradiation method has been widely applied for the synthesis of mesoporous materials [11–13]. Compared with the hydrothermal synthesis method, the microwave irradiation technique performed several fascinating advantages, such as heated system with uniform temperature, molecular selective heating, and without hysteresis, which resulting in more homogeneous nucleation and rapid crystallization. However, most investigations of microwave irradiation were aimed at synthesizing pure silica MCM-41 molecular sieve. Few reports [14–16] were presented concerning to the mesoporous molecular sieve modified with heteroatoms under microwave irradiation.

Diphenyl carbonate (DPC) is an important organic compound as a raw material for non-phosgene production of polycarbonate. In order to satisfy the increasing demands for safe and clean processes, the traditional phosgene process for DPC based on the reaction of phenol and phosgene in the presence of bases [17] must be abandoned. It is believed that the transesterification of dimethyl oxalate (DMO) with phenol to diphenyl oxalate (DPO) followed by decarbonylation of DPO to DPC is a promising green route for DPC synthesis [18]. The reaction between phenol and DMO follows two steps, viz. the transesterification of DMO with phenol into methyl phenyl oxalate (MPO) and the disproportion of MPO to DPO. A variety of catalyst systems have been developed for the

* Corresponding author. Tel.: +86 22 87401818; fax: +86 22 87401818.
** Corresponding author. Tel.: +86 22 27406498; fax: +86 22 87401818.
E-mail addresses: spwang@tju.edu.cn (S. Wang), xbma@tju.edu.cn (X. Ma).

1385-8947/$ – see front matter © 2010 Elsevier B.V. All rights reserved.
doi:10.1016/j.cej.2010.11.081

transesterification reaction, which include homogeneous catalyst such as Lewis acids or soluble organic Pb, Sn, or Ti compounds and heterogeneous catalysts such as $MoO_3/TiO_2–SiO_2$, TiO_2/SiO_2, Ti-containing phosphate catalysts, cyclopentadienyl-functionalized materials, etc. [19–22].

In this paper, the synthesis of titanium-containing mesoporous materials (Ti-MCM-41) was achieved under a microwave irradiation condition. In particular, we focused to research the influence of heating temperature on their physicochemical properties. The samples prepared by microwave irradiation method and hydrothermal method respectively have been compared for both textural characteristics and catalytic performance. Various characterization techniques, including XRD, FT-IR, N_2 adsorption and desorption, DRUV–vis, NH_3–TPD and particle size analysis were carried out to investigate the structure and surface properties of these samples. The catalytic properties of these materials were tested for the transesterification of dimethyl oxalate and phenol.

2. Experimental

2.1. Catalyst synthesis

The titanium-containing mesoporous materials were prepared under a microwave-irradiation condition using cationic surfactant cetyltrimethylammonium bromide (CTAB) as a template. Tetraethyoxysilane (TEOS) and tetrabutyl titanate (TBOT) were used as Si and Ti sources, respectively. The synthesis of titanosilicate gel was carried out as follows: 3.64 g of CTAB were dissolved in 90 mL of deionized water under vigorous stirring at 313 K, and then 15.32 g of TEOS was added dropwise to the surfactant solution followed by pH adjustment to 11.0 through gradually addition of NaOH solution. After 10 min, 0.50 g TBOT dissolved in isopropyl alcohol (i-PrOH) was then dropped into the mixture. The stirring was maintained for 40 min for the sufficient hydrolysis of TEOS and TBOT. The pH value of mixed solution adjusted by NaOH solution was between 10.5 and 11.0. The molar composition of final gel was CTAB: 7.35TEOS: 0.147TBOT: 1.5NaOH: $500H_2O$: 7.35i-PrOH. The resulting suspension was transferred into Teflon vessels and heated via non-pulsed microwave irradiation in a Multiwave 3000 microwave reaction system (Anton Paar) which equipped with an 8-rotor tray. Making use of a temperature sensor, a pressure sensor and an adjustable power output (maximum 1200 W), microwave system provided a way for rapid uniform heating. Crystallization was performed in the temperature controlled mode that the temperature was ramped for 5 min and hold 40 min at different temperature varied from 353 K to 413 K. The maximum pressure increase rate was set at 0.3 bar s^{-1}; the maximum pressure in the reaction vessels was programmed to not exceed 2 MPa. After cooling to room temperature, the solid products were isolated by filtering, washed with deionized water, and dried in air at 373 K for 12 h. To remove the organic species, the dried samples were calcined at 823 K for 6 h in air with a heating rate of 2 K/min. The samples prepared under the microwave irradiation condition were designated as Ti-MCM-41-Mxxx, xxx was the temperature of microwave crystallization, e.g. Ti-MCM-41-M353, represented the sample prepared by microwave irradiation at 353 K. The pure silica MCM-41 material was also synthesized under the microwave irradiation condition at 393 K according to the procedure described above, and designated as MCM-41-M393.

In contrast, the conventional hydrothermal synthesis method was also carried out in this work. The hydrothermal synthesis was accomplished in a 150-mL Teflon-lined autoclave heating at 373 K for 1 day. After calcinations, the samples obtained through hydrothermal synthesis were designated Ti-MCM-41-H.

2.2. Catalyst characterization

The samples obtained through above methods were characterized by several instrumental analysis techniques. The Ti content in the final products was analyzed by an inductively coupled plasma optical emission spectrometry (ICP-OES) (Varian, Vista-MPX). The determination was operated at a high frequency emission power of 1.5 kW and a plasma airflow of 15.0 L/min (λ_{Ti} = 336.122 nm). The crystallinity of the samples was measured by X-ray powder diffraction (XRD) on a Rigaku D/max-2500 diffractometer with graphite filtered Cu Kα radiation (λ = 0.154056 nm) at 40 kV and 100 mA. Diffraction data were recorded at an interval of 0.01° and a scanning speed of 4° min^{-1} from $2\theta = 1°$ to $2\theta = 10°$. Specific surface area, pore size distribution and total pore volume were determined by N_2 adsorption–desorption isotherms obtained at 77 K by the use of a Tristar 3000 surface area and porosity analyzer (Micrometritics). The samples were previously degassed at 573 K for 3 h at vacuum. The surface area was calculated by the Brunauer–Emmet–Teller (BET) method and the pore size distribution was determinated applying the Barrett–Joyner–Halenda (BJH) method, based on the Kelvin equation [23]. Fourier transform infrared (FT-IR) spectra of samples were recorded on a Nicolet 6700 spectrometer (Nicolet) with KBr pellet technique. The effective region was from 400 to 4000 cm^{-1}. The nature of Ti species was determined by diffuse reflectance UV–visible (DRUV–vis) spectroscopy. The measurement was performed at room temperature using a UV-3600 spectrometer (Shimazu) in the wavelength range of 190–700 nm. FTIR measure of pyridine adsorbed was carried out on a Nicolet 6700 spectrometer (Nicolet) with a 4 cm^{-1} resolution and a 4000–400 cm^{-1} scanning range. The sample was pressed into a self-supporting wafer followed by evacuation at 623 K for 0.5 h. After cooled down to 333 K, the pyridine was adsorbed. The spectra were recorded after the sample temperature held for 0.5 h. NH_3-TPD experiments were conducted on Auto-chem 2910 chemical adsorption instrument (Micromeritics). The samples were heated to 823 K in flowing He (30 mL/min) for 1 h, and then cooled to room temperature. Adsorption of ammonia was carried out at 323 K to saturation. Ammonia was replaced with helium and desorption was monitored by increasing temperature from 323 K to 873 K at a rate of 10 K min^{-1}. Particle size distribution was examined by a zetaPALS zeta potential analyzer (Brookhaven).

2.3. Transesterification of DMO with phenol

The transesterification reaction of DMO with phenol was conducted in a three-necked round bottomed flask (125 mL) equipped with a thermometer, a condenser, and a magnetic stirrer under refluxing condition at atmospheric pressure with Ti-MCM-41 as catalyst. The condenser consisted of a distillation column kept at 353 K by flowing recycled hot water to remove methanol by-product from the reaction system. Thus, the reaction was accelerated towards the desired direction. DMO and phenol were added into the batch reactor with a molar ratio of 1:3. Then nitrogen gas was flowed at 30 sccm for 10 min to purge the air from the reaction system. The reaction temperature was kept at 453 K, and the reaction time was 2 h. Quantitative analysis of reaction products was performed on an HP1100 series high-performance liquid chromatography (Agilent Technologies) equipped with a quaternary gradient pump, an online degasser and an ultraviolet visible detector (VWD). A ZORBAX Eclipse XDB-C18 column (150 mm × 4.6 mm, 5 μm, Agilent Technologies) was used for the liquid-chromatographic analysis of the products. The separation was achieved under a step-gradient elution condition with a mixed mobile phase consisting of water and acetonitrile and the UV detection at 254 nm at atmospheric temperature.

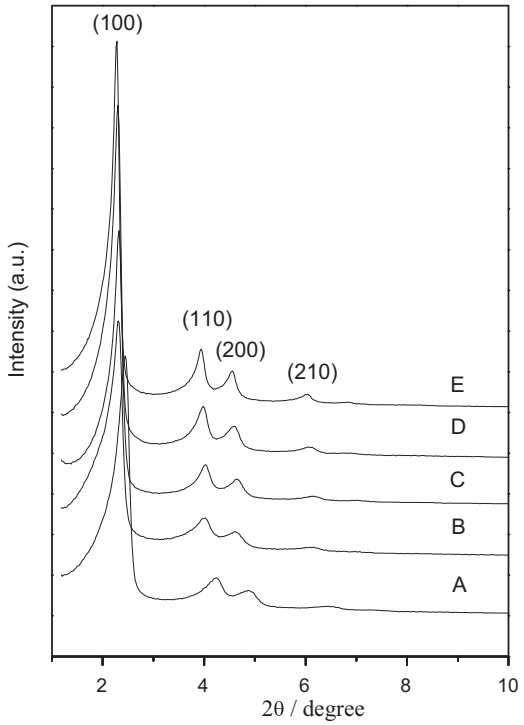

Fig. 1. XRD patterns of Ti-MCM-41 samples synthesized by microwave-irradiation method according to the microwave heating temperature ((A) 353 K, (B) 373 K, (C) 393 K, (D) 413 K) and hydrothermal method (E).

3. Results and discussion

3.1. XRD

The XRD patterns of Ti-MCM-41 samples synthesized under different crystallization conditions are shown in Fig. 1. The interplanar distance (d_{100}) and the hexagonal unit cell parameter (a_0) of the samples, estimated by XRD, are summarized in Table 1. As showed in Fig. 1 and Table 1, all the samples exhibit four well-defined peaks including a main reflection peak corresponding to the (1 0 0) plane at a low angle (around $2\theta = 2–3^\circ$) and other three weak peaks which can be indexed with (1 1 0), (2 0 0), (2 1 0) planes at region of $2\theta = 3–7^\circ$; no diffractions were seen at higher angles. It is indicated that the samples have typical long-range order of hexagonal MCM-41 structure [1]. As the temperature of microwave heating increases, the XRD peaks become more intense and sharper, implying the more degree of long-range order. In addition, the XRD peaks slightly shift towards lower diffraction angle, and parameter a_0 increases a little in the range of 4.0–4.5 nm with the increase of the microwave heating temperature. This should be correlated to a probable incorporation of Ti atoms into framework. As reported by the others [24], due to differences in the ionic radius of Ti^{4+} (0.068 nm) and Si^{4+} (0.041 nm), the substitution of the larger Ti^{4+} ion in place of Si^{4+} invariably should distort the geometry around Ti from an ideal tetrahedral coordination. Thus, when a certain amount Ti atoms penetrated into framework (Ti–O bond length 0.179 nm) and replaced Si atoms (Si–O bond length 0.161 nm), there should be some structure deformation, expressing a low-angle shift of XRD peaks and a increasing of the unit lattice. It can be seen from Fig. 1 that the temperature of microwave irradiation could affect the incorporation of titanium into the structure as well as the degree of organization of Ti-MCM-41. And the XRD patterns of the samples prepared by microwave heating do not show significant difference from that obtained from conventional hydrothermal heating.

3.2. N_2 adsorption–desorption isotherms

Fig. 2(a) illustrates the N_2 adsorption–desorption isotherms of the synthesized samples. The specific surface areas, average pore size and pore volumes are listed in Table 1. All the samples exhibit typical type IV isotherms (definition by IUPAC) with hysteresis loop caused by capillary condensation in mesopores, which is a characteristic for mesoporous materials [25]. As showed in Fig. 2(a), the adsorption at low relative pressure ($P/P^\circ < 0.2$) is occurred from monolayer adsorption of N_2, following multilayer adsorption on the walls of mesopores. All the isotherms show a sharp inflection at a relative pressure of 0.25–0.35 characteristic of capillary condensation inside the primary mesopores, showing that all the samples have typical mesostructure with uniform pore size distribution and large pore volumes [26]. Meanwhile, a pronounced hysteresis loop with a sharp increase in the adsorption branch at

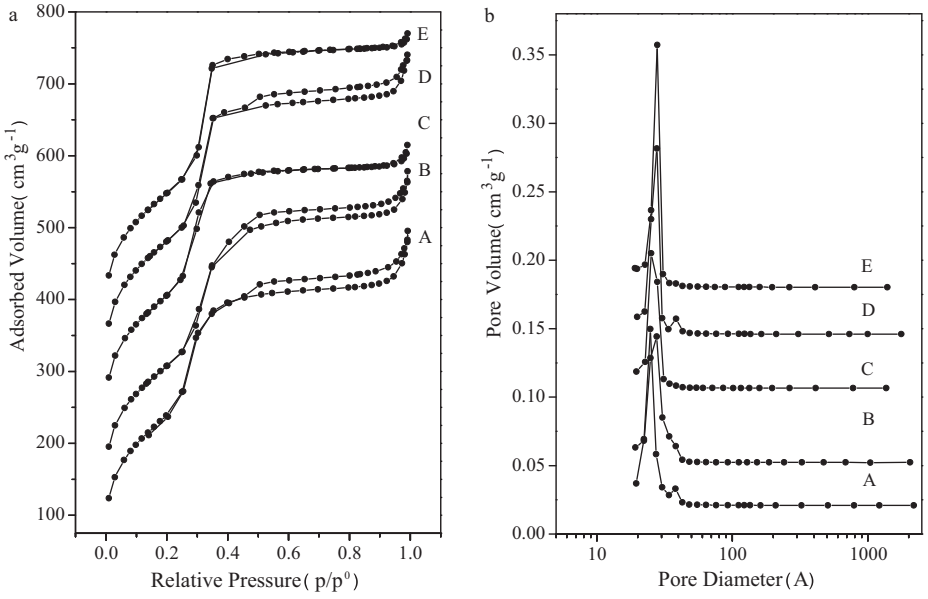

Fig. 2. Nitrogen adsorption–desorption isotherms (a) and pore size distribution curves (b) of the Ti-MCM-41 samples synthesized by microwave-irradiation method according to the microwave heating temperature ((A) 353 K, (B) 373 K, (C) 393 K, (D) 413 K) and hydrothermal method (E).

Table 1
Chemical composition and textural properties of Ti-MCM-41 samples prepared by microwave-irradiation method and hydrothermal method.

Samples	Ti content[a] (wt. %)	2θ (1 0 0) (°)	$d_{1\,0\,0}$ (Å)	a_0 (Å)	S_{BET} (m^2/g)	Average pore size (Å)	Pore volume (cm^3/g)
Ti-MCM-41-M353	1.48	2.44	36.2	41.8	840	29.3	0.854
Ti-MCM-41-M373	1.52	2.30	38.4	40.2	876	30.4	0.867
Ti-MCM-41-M393	1.54	2.32	38.1	44.0	896	28.6	0.839
Ti-MCM-41-M413	1.53	2.30	38.4	44.3	884	29.9	0.858
Ti-MCM-41-H	1.53	2.30	38.4	44.4	890	28.2	0.806

[a] Elemental content in final products measured by ICP analysis.

relative pressure about 0.9 could be due to a capillary condensation in secondary mesopores. According to literatures [27–29], those secondary mesoporosity refers to some interparticle pores or some significant large cavities.

In addition, as shown in Fig. 2(b), the narrow and sharp peaks can be observed in an average pore size range of 25–28 Å, revealing that the samples have uniform pore size distribution. Furthermore, as for Ti-MCM-41-M393, similar as Ti-MCM-41-H, there is a single peak in its pore size distribution curve. Associated to Fig. 2(a), the other samples express more pronounced hysteresis loops and much sharper and higher inflection approaching saturation vapor pressure than Ti-MCM-41-M393 and Ti-MCM-41-H, indicating a larger number of secondary mesopores. Owing to a narrow and uniform pore size distribution, Ti-MCM-41-M393 has a smaller average pore size (28.6 Å) and a higher surface area (896 m^2/g) than any other Ti-MCM-41-M samples listed in Table 1.

3.3. FTIR and ICP-OES

Fig. 3 shows the FT-IR spectra in 400–1400 cm^{-1} range for KBr-pelletized Ti-MCM-41 samples. The broad band at 1087 cm^{-1}, with a shoulder at 1250 cm^{-1} and the band 807 cm^{-1} are assigned to asymmetric and symmetric stretching vibration of Si–O–Si bonds, respectively [30,31]. The band at 450 cm^{-1} is attributed to tetrahedral bending vibration of Si–O–Si bonds. It has been demonstrated that the band at about 960 cm^{-1} could be ascribed to the stretching vibration of SiO_4 tetrahedra bonded to a titanium atom through Si–O–Ti bonds [32,33]. However, this absorption band is sometimes associated with silanol groups (Si–OH) at the defect sites. Thus, this band can be assigned to the overlapping of both Si–OH groups and Si–O–Ti bonds vibrations. As shown from Fig. 3, with the increase of microwave heating temperature up to 393 K, the strength of 960 cm^{-1} band enhanced gradually. In order to exclude the contribution of OH region, the infrared spectra in the 3300–3900 cm^{-1} range for Ti-MCM-41 samples have been investigated (not exhibited). A clear band at 3750 cm^{-1} is observed in all of synthesized samples due to the stretching vibration of isolated Si–OH groups, located mainly at the surface of the inner walls of the MCM-41 channels [34]. Its intensity remains almost unchanged for all of the samples synthesized in different conditions, indicating that the amount of silanol groups would not be affected by synthesis condition.

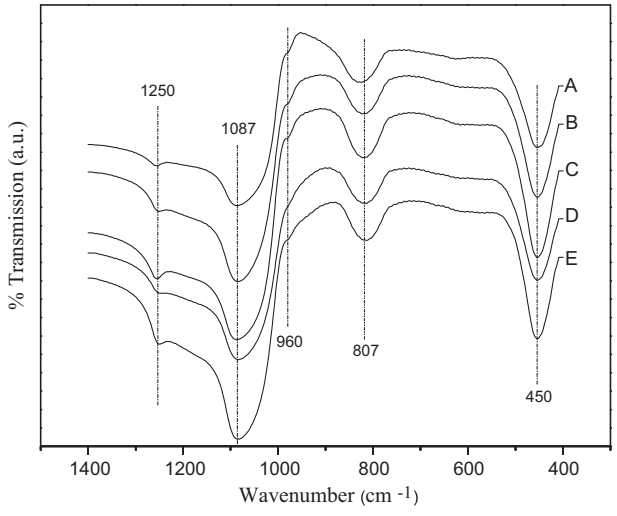

Fig. 3. FT-IR spectra of Ti-MCM-41 samples synthesized by microwave-irradiation method according to the microwave heating temperature ((A) 353 K, (B) 373 K, (C) 393 K, (D) 413 K) and hydrothermal method (E).

Additionally, Table 1 summarizes the element contents of Ti in Ti-MCM-41 samples, which is accomplished by ICP-OES analysis. It can be seen that the samples synthesized under different condition differ from each other in the actual Ti content. The content of Ti in samples shows a gradually increasing trend as microwave heating temperature is raised. The maximal value is 1.54% until the temperature reaches 393 K, after which the Ti content drops somewhat.

Considering the above results, the variation of the 960 cm^{-1} band intensity could be associated with titanium incorporation into the silica framework in tetrahedral positions. The strength of 960 cm^{-1} band increases along with the heating temperature, suggesting that raising temperature is benefit to enhance Ti substitution in the mesoporous silica framework.

3.4. DRUV–vis

DRUV–vis spectroscopy is a very sensitive method for characterization of the coordination environment of titanium in zeolite framework [35–37]. The DRUV–vis spectra of Ti-MCM-41 samples are shown in Fig. 4. All the samples have an intense band centered at 210 nm attributed to a low-energy charge-transfer transition from tetrahedral oxygen ligands to central Ti^{4+} ions, indicating that most of the Ti species are isolated and in tetrahedral coordination inside the framework [38,39]. Another band observed at the region of 260–280 nm suggests the presence of small amounts of polymerized Ti–O–Ti species in a higher coordination (such as penta-, hexa- or octahedral coordinated Ti species) coexisting with the tetrahedral Ti sites [40,41]. The absence of an absorption band characteristic of octahedral extra-framework titanium at about 330 nm in all samples implies that there is no separated anatase-like titania phase formed during the preparation [39,42]. Obviously, the tetrahedral component of Ti(IV) is prevalent in Ti-MCM-41 synthesized under microwave irradiation condition. Comparably, there is no significant difference between the samples prepared in two different routes. The DRUV–vis spectra of Ti-MCM-41 synthesized in this study confirm that Ti atoms have entirely substituted into the silica framework.

3.5. Particle size distribution

Fig. 5 shows the particle size distribution curves of the titanium-containing mesoporous materials. The average particle sizes of the samples prepared by microwave irradiation distribute at 480–530 nm, while that prepared by hydrothermal method is 665 nm. Additionally, the samples prepared by microwave heat-

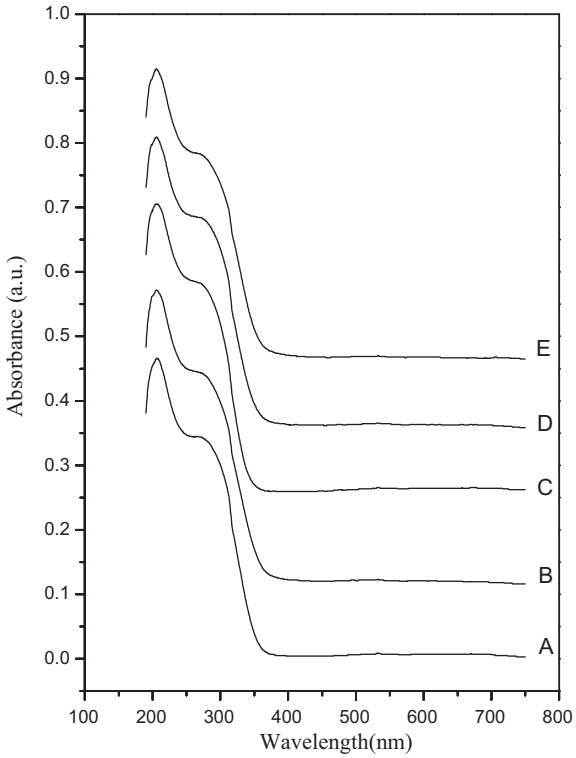

Fig. 4. UV–visible diffuse reflectance spectra of Ti-MCM-41 samples synthesized by microwave-irradiation method according to the microwave heating temperature ((A) 353 K, (B) 373 K, (C) 393 K, (D) 413 K) and hydrothermal method (E).

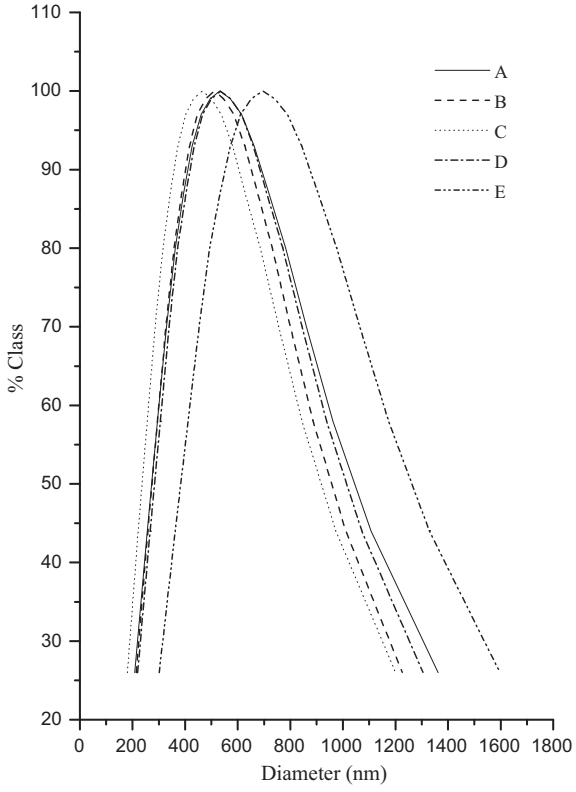

Fig. 5. Particle size distribution of Ti-MCM-41 samples synthesized by microwave-irradiation method according to the microwave heating temperature ((A) 353 K, (B) 373 K, (C) 393 K, (D) 413 K) and hydrothermal method (E).

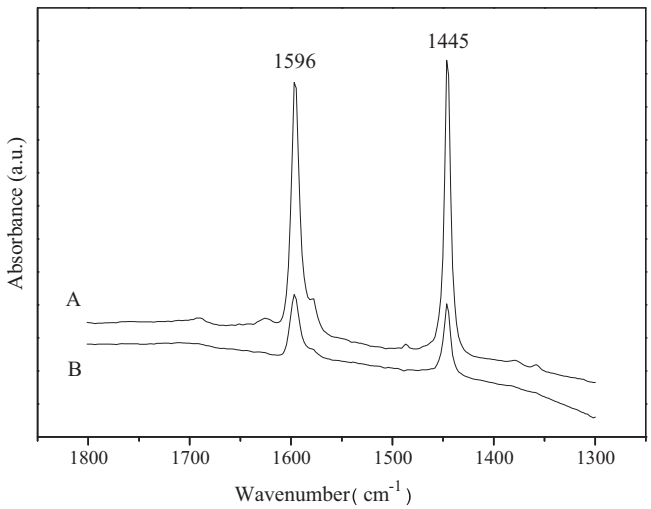

Fig. 6. FTIR spectra of pyridine adsorbed on Ti-MCM-41-M393 (A) and MCM-41-M393 (B) after desorption at 333 K.

ing exhibit narrower particle size distribution. It would probably be resulted by the homogeneous and quick heating in microwave irradiation [43]. As shown in Fig. 5, Ti-MCM-41 samples become smaller with microwave heating temperature increases at a limit of 393 K. And then it becomes bigger with further improving the temperature to 413 K. Thus, there is a consequence that excessive heating would lead to an aggregation of the particles. Moreover, this conclusion would agree with the results from N_2 adsorption–desorption isotherms. As shown in Fig. 3, the formation of large secondary mesopores could be due to the aggregation of large particles.

3.6. Pyridine-FTIR and NH_3-TPD

As reported [44], the acidity of pure silica MCM-41 is very poor. However, the incorporation of heteroatoms to the pure siliceous framework, such as titanium, may generate acid sites. FT-IR measure of adsorbed pyridine has been performed to distinct the nature of acidic sites (Lewis and Brönsted) on the surface of the catalysts. Fig. 6 shows the FTIR spectra of adsorbed pyridine on Ti-MCM-41-393 and MCM-41-M393, respectively. The samples show two bands at around 1596 cm^{-1} and 1445 cm^{-1}, respectively. The band at 1596 cm^{-1} can be attributed to hydrogen-bonded pyridine [45]. The band at 1445 cm^{-1} corresponds to vibration of pyridine chemisorbed on the Lewis acid sites [46]. Brönsted acid sites (peaks at about 1540 cm^{-1}) are absent. It is obvious that the IR absorption bands on the surface of Ti-MCM-41 are more intense than those of the pure silica MCM-41. Due to the Ti-incorporation into the pure silica framework, the surface silanol groups are activated and form hydrogen bonds with pyridine, whose hydroxyls are not capable enough to protonate pyridine. Meanwhile, the Ti species incorporated in the framework, could adsorb pyridine coordinatively as Lewis acid sites on the surface of Ti-MCM-41.

Ammonia TPD characterization is a well-known method for determination of surface acid strength of solid heterogeneous catalysts. In the NH_3-TPD curves, peaks are generally distributed into two regions: below and above 673 K referred to as low-temperature (LT) and high-temperature (HT) regions, respectively. The peaks in the HT region can be attributed to desorption of NH_3 from strong Brönsted and Lewis type acid sites, and the peaks in the LT region is assigned as the desorption of NH_3 from weak acid sites [47,48]. From the results shown in Fig. 7, it can be seen that the peaks only appear in the low temperature region, confirming that there only exist weak acid sites on the surface of these

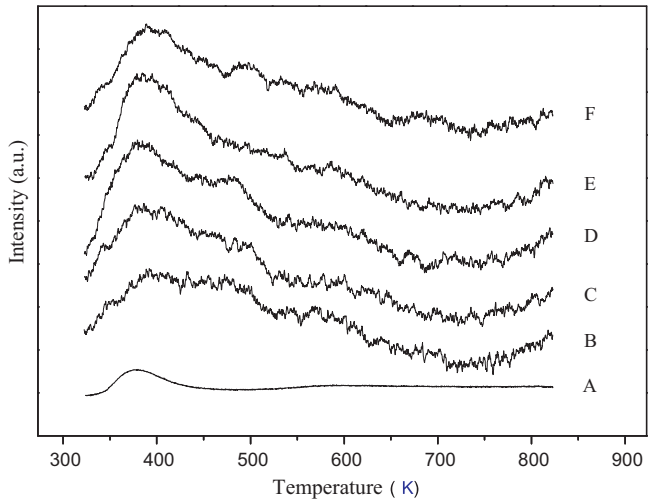

Fig. 7. NH_3-TPD profile of MCM-41-M393 (A), Ti-MCM-41 samples synthesized by microwave-irradiation method according to the microwave heating temperature ((B) 353 K, (C) 373 K, (D) 393 K, (E) 413 K) and hydrothermal method (F).

mesoporous materials. For the pure MCM-41, the ammonia desorbs in a low temperature region below 423 K; however, for the Ti-MCM-41 samples prepared through different routes, not only the amount of ammonia adsorbed but also the desorption temperature increases intensely. It means that the incorporation of Ti into the silica framework enhance the acidity of the mesoporous materials. Moreover, for the Ti-MCM-41 samples prepared by microwave irradiation method, the band of NH_3 desorbed becomes more intense with the increasing microwave irradiation temperature from 353 K to 393 K, and then weakens at 413 K, implying that the temperature has a notable impact on the amount of the surface acid sites of Ti-MCM-41 and more acid sites were obtained on the surface of Ti-MCM-41-M393. According to the chemical composition of the samples listed in Table 1, Ti content of the samples synthesized by microwave irradiation method raises gradually along with temperature increase. In addition, associated with the results of FT-IR and DRUV–vis spectroscopy, the increasing temperature could prompt titanium to incorporate into the silica framework, and brings about the increasing amount of weak acid sites on the surface of Ti-MCM-41. However, excessive temperature is disadvantageous for Ti substitution in the silica framework. The optimal temperature for microwave irradiation is 393 K.

3.7. Transesterification catalytic performances

Table 2 shows the comparative results of catalytic properties of a series of Ti-MCM-41 catalysts prepared by hydrothermal and microwave irradiation method with different temperature for the transesterification of DMO with phenol. The pure MCM-41 catalyst displayed poor catalytic properties with the DMO conversion of 14.4%, and the DPO yield of only 0.43%. However, all the Ti-MCM-41 catalysts are active for the reaction, giving the conversion of DMO over 42%. The samples synthesized using microwave irradiation, e.g. those heated up 373 K, could perform in somewhat more excellently than that prepared by hydrothermal method. It is possibly due to the narrower particle size distribution and the smaller particle size, as diffusion plays an important role in liquid-phase reaction. The shorter channels in the small size particles accelerated the diffusion rate of reactants/products, thus the accessibility to the catalytic center is enhanced greatly [49]. In addition, microwave heating temperature gives a significant effect to the catalytic activities of Ti-MCM-41. The DMO conversion increased steadily with heating temperature increased up to 393 K, as well as the yield of DPO, and then decreased at a higher temperature 413 K. The best performance has been shown over Ti-MCM-41-M393, where DMO conversion, DPO selectivity and yield reached the maximum values of 55.3%, 17.3%, 9.6%, respectively. As reported previously [50], TiO_2/SiO_2 was an active catalyst for the synthesis of DPO from the transesterification of DMO with phenol. However, unless the Ti loading reached 8%, the catalytic activities of TiO_2/SiO_2 was lower than that of Ti-MCM-41-M393, whose Ti content was just 1.54%. The desirable catalytic activities of Ti-MCM-41-M393 could be ascribed to the following factors: (1) the rich Ti(IV) active centers which provide more weak Lewis acid sites; (2) the well-ordered structure of mesoporous molecular sieve with a large BET surface area; (3) a small particle diameter.

Table 2
Activities of catalysts for the transesterification of dimethyl oxalate with phenol.

Samples	Conversion (%)	Selectivity (%)		Yield (%)	
		DPO	MPO	DPO	MPO
Ti-MCM-41-M353	44.5	10.7	89.3	4.8	39.7
Ti-MCM-41-M373	54.4	16.1	83.9	8.8	45.7
Ti-MCM-41-M393	55.3	17.3	82.7	9.6	45.7
Ti-MCM-41-M413	54.5	16.6	83.4	9.1	45.4
MCM-41-M393	14.4	2.99	97.0	0.43	14.0
Ti-MCM-41-H	49.4	14.9	85.1	7.4	42.1

4. Conclusions

In conclusion, titanium-containing mesoporous materials were synthesized successfully by microwave irradiation method. One of the advantages of the microwave irradiation method is that the well-ordered mesoporous structure could be achieved within a short crystallization time. By means of XRD, FT-IR, N_2 adsorption and desorption, DRUV–vis, pyridine-FTIR, NH_3-TPD and particle size analysis, it indicated that Ti-MCM-41 samples prepared by microwave irradiation method and hydrothermal method, respectively, have similar structural and textural properties. There is a consequence that the samples prepared by microwave irradiation showed the typical long-range order of hexagonal MCM-41 structure with a high surface area and an average pore diameter of about 3 nm. Merging the results from FT-IR, DRUV–vis and ICP analysis, it was confirmed that Ti has been incorporated into the silica framework mainly in tetrahedral isolated sites. Meanwhile, the amounts of Ti species increased slightly as the synthesis temperature was raised, and the maximal value appeared at 393 K. The temperature of microwave irradiation could affect the incorporation of titanium into the structure as well as the degree of organization of Ti-MCM-41. These mesoporous Ti-MCM-41 prepared using microwave method were active for transesterification of DMO and phenol and the optimal heating temperature is 393 K. The small particle size, large surface area and plenty of Ti(IV) active centers inside the framework, which provide more weak acid sites, are advantageous to enhance the catalytic properties.

Acknowledgements

Financial supports by Natural Science Foundation of China (NSFC) (Grant No. 20506018), the Program of Introducing Talents of Discipline to Universities (Grant B06006), the National Key Project for the 11th Five Year Plan (Grant No. 2006BAE02B00), and the Program for New Century Excellent Talents in University (NCET-04-0242) are gratefully acknowledged.

References

[1] J.S. Beck, J.C. Vartuli, W.J. Roth, M.E. Leonowicz, C.T. Kresge, K.D. Schmitt, C.T.W. Chu, D.H. Olson, E.W. Sheppard, A new family of mesoporous molecu-

lar sieves prepared with liquid crystal templates, J. Am. Chem. Soc. 114 (1992) 10834–10843.
[2] R.K. Rana, B. Viswanathan, Mo incorporation in MCM-41 type zeolite, Catal. Lett. 52 (1998) 25–29.
[3] Q. Luo, F. Deng, Z.Y. Yuan, J. Yang, M.J. Zhang, Y. Yue, C.H. Ye, Using trimethylphosphine as a probe molecule to study the acid states in Al-MCM-41 materials by solid-state NMR spectroscopy, J. Phys. Chem. B 107 (2003) 2435–2442.
[4] T. Blasco, A. Corma, M.T. Navarro, J.P. Pariente, Synthesis, characterization, and catalytic activity of Ti-MCM-41 structures, J. Catal. 156 (1995) 65–74.
[5] C. Galacho, M.M.L.R. Carrott, P.J.M. Carrott, Structural and catalytic properties of Ti-MCM-41 synthesised at room temperature up to high Ti content, Micropor. Mesopor. Mater. 100 (2007) 312–321.
[6] M. Guidotti, I. Batonneau-Gener, E. Gianotti, L. Marchese, S. Mignard, R. Psaro, M. Sgobba, N. Ravasio, The effect of silylation on titanium-containing silica catalysts for the epoxidation of functionalised molecules, Micropor. Mesopor. Mater. 111 (2008) 39–47.
[7] P. Wu, M. Iwamoto, Metal-ion-planted MCM-41. Part 3. Incorporation of titanium species by atom-planting method, J. Chem. Soc. Faraday Trans. 94 (1998) 2871–2875.
[8] L.Y. Chen, S. Jaenicke, G.K. Chuah, Thermal and hydrothermal stability of framework-substituted MCM-41 mesoporous materials, Micropor. Mater. 12 (1997) 323–330.
[9] M. Anpo, H. Yamashita, K. Ikeue, Y. Fujii, S.G. Zhang, Y. Ichihashi, D.R. Park, Y. Suzuki, K. Koyano, T. Tatsumi, Photocatalytic reduction of CO_2 with H_2O on Ti-MCM-41 and Ti-MCM-48 mesoporous zeolite catalysts, Catal. Today 44 (1998) 327–332.
[10] Y.W. Chen, H.Y. Lin, Characteristics of Ti-MCM-41 and its catalytic properties in oxidation of benzene, J. Porous Mater. 9 (2002) 175–184.
[11] S.E. Park, D.S. Kim, J.S. Chang, W.Y. Kim, Synthesis of MCM-41 using microwave heating with ethylene glycol, Catal. Today 44 (1998) 301–308.
[12] E.B. Celer, M. Jaroniec, Temperature-programmed microwave-assisted synthesis of SBA-15 ordered mesoporous silica, J. Am. Chem. Soc. 128 (2006) 14408–14414.
[13] Y.K. Hwang, J.S. Chang, Y.U. Kwon, S.E. Park, Microwave synthesis of cubic mesoporous silica SBA-16, Micropor. Mesopor. Mater. 68 (2004) 21–27.
[14] C. Wu, Q. Gao, J. Hu, Z. Chen, W. Shi, Rapid preparation, characterization and hydrogen storage properties of pure and metal ions doped mesoporous MCM-41, Micropor. Mesopor. Mater. 117 (2009) 165–169.
[15] C.F. Cheng, H.H. Cheng, L.L. Wu, B.W. Cheng, Synthesis and characterization of nanoscale aluminosilicate mesoporous materials by microwave irradiation, Nanoporous Mater. 156 (2005) 113–118.
[16] T.S. Jiang, Y.J. Tang, Q. Zhao, H.B. Yin, Effect of Ni-doping on the pore structure of pure silica MCM-41 mesoporous molecular sieve under microwave irradiation, Colloid Surf. A 315 (2008) 299–303.
[17] J.L. Gong, X.B. Ma, S.P. Wang, Phosgene-free approaches to catalytic synthesis of diphenyl carbonate and its intermediates, Appl. Catal. A Gen. 316 (2007) 1–21.
[18] Y. Liu, X. Ma, S. Wang, J. Gong, The nature of surface acidity and reactivity of MoO_3/SiO_2 and MoO_3/TiO_2–SiO_2 for transesterification of dimethyl oxalate with phenol: a comparative investigation, Appl. Catal. B Environ. 77 (2007) 125–134.
[19] K. Nishihira, S. Tanaka, Y. Nishida, I. Hirofumi, S. Fujitsu, K. Harada, R. Sugise, K. Kashiwagi, T. Doi, US 5,811,573, 1998.
[20] S.P. Wang, Y. Liu, Y. Shi, X.B. Ma, J.L. Gong, Dispersion, catalytic activity of MoO_3 on TiO_2–SiO_2 binary oxide support, AIChE J. 54 (2008) 741–749.
[21] X. Yang, X.B. Ma, S.P. Wang, J.L. Gong, Transesterification of dimethyl oxalate with phenol over TiO_2/SiO_2: catalyst screening and reaction optimization, AIChE J. 54 (2008) 3260–3272.
[22] G.M. Zhao, X.M. Zhu, Z.L. Wang, G. Liu, Y. Liu, M.J. Jia, W.X. Zhang, Transesterification of dimethyl oxalate with phenol over Ti-containing phosphate catalysts, React. Kinet. Catal. Lett. 91 (2007) 77–83.
[23] E.P. Barrett, L.G. Joyner, P.P. Halenda, The determination of pore volume and area distributions in porous substances. I. Computations from nitrogen isotherms, J. Am. Chem. Soc. 73 (1951) 373–380.
[24] H. Kosslick, G. Lischke, H. Landmesser, B. Parlitz, W. Storek, R. Fricke, Acidity and catalytic behavior of substituted MCM-48, J. Catal. 176 (1998) 102–114.
[25] M. Kruk, M. Jaroniec, Gas adsorption characterization of ordered organic –inorganic nanocomposite materials, Chem. Mater. 13 (2001) 3169–3183.
[26] B.S. Uphade, Y. Yamada, T. Akita, T. Nakamura, M. Haruta, Synthesis and characterization of Ti-MCM-41 and vapor-phase epoxidation of propylene using H_2 and O_2 over Au/Ti-MCM-41, Appl. Catal. A Gen. 215 (2001) 137–148.
[27] M. Kruk, M. Jaroniec, Y. Sakamoto, O. Terasaki, R. Ryoo, C.H. Ko, Determination of pore size and pore wall structure of MCM-41 by using nitrogen adsorption, transmission electron microscopy, and X-ray diffraction, J. Phys. Chem. B 104 (2000) 292–301.
[28] M. Kruk, M. Jaroniec, R. Ryoo, J.M. Kim, Characterization of high-quality MCM-48 and SBA-1 mesoporous silicas, Chem. Mater. 11 (1999) 2568–2572.
[29] T.S. Jiang, W. Shen, Q. Zhao, M. Li, J.Y. Chu, H.B. Yin, Characterization of CoMCM-41 mesoporous molecular sieves obtained by the microwave irradiation method, J. Solid State Chem. 181 (2008) 2298–2305.
[30] Y. Kong, H.Y. Zhu, G. Yang, X.F. Guo, W.H. Hou, Q.J. Yan, M. Gu, C. Hu, Investigation of the structure of MCM-41 samples with a high copper content, Adv. Funct. Mater. 14 (2004) 816–820.
[31] R. Takahashi, S. Sato, T. Sodesawa, M. Kawakita, K. Ogura, High surface-area silica with controlled pore size prepared from nanocomposite of silica and citric acid, J. Phys. Chem. B. 104 (2000) 12184–12191.
[32] V. Lafond, P.H. Mutin, A. Vioux, Control of the texture of titania-silica mixed oxides prepared by nonhydrolytic sol–gel, Chem. Mater. 16 (2004) 5380–5386.
[33] M.R. Prasad, G. Madhavi, A.R. Rao, S.J. Kulkarni, K.V. Raghavan, Synthesis, characterization of high Ti-containing Ti-MCM-41 catalysts and their activity evaluation in oxidation of cyclohexene and epoxidation of higher olefins, J. Porous Mater. 13 (2006) 81–94.
[34] M.P. Wagner, Reinforcing silicas and silicates, Rubber Chem. Technol. 49 (1976) 703–774.
[35] S. Bordiga, S. Coluccia, C. Lamberti, L. Marchese, A. Zecchina, F. Boscherini, F. Buffa, F. Genoni, G. Leofanti, XAFS study of Ti-silicalite: structure of framework Ti(IV) in the presence and absence of reactive molecules (H_2O, NH_3) and comparison with ultraviolet–visible and IR results, J. Phys. Chem. 98 (1994) 4125–4132.
[36] G. Ricchiardi, A. Damin, S. Bordiga, C. Lamberti, G. Spano, F. Rivetti, A. Zecchina, Vibrational structure of titanium silicate catalysts. A spectroscopic and theoretical study, J. Am. Chem. Soc. 123 (2001) 11409–11419.
[37] J.A. Melero, J.M. Arsuaga, P.d. Frutos, J. Iglesias, J. Sainz, S. Blázquez, Direct synthesis of titanium-substituted mesostructured materials using non-ionic surfactants and titanocene dichloride, Micropor. Mesopor. Mater. 86 (2005) 364–373.
[38] G.A. Eimer, C.M. Chanquia, K. Sapag, E.R. Herrero, The role of different parameters of synthesis in the final structure of Ti-containing mesoporous materials, Micropor. Mesopor. Mater. 116 (2008) 670–676.
[39] V.N. Rajakovic, S. Mintova, J. Senker, T. Bein, Synthesis and characterization of V- and Ti-substituted mesoporous materials, Mater. Sci. Eng. C 23 (2003) 817–821.
[40] D.T. On, S.V. Nguyen, V. Hulea, E. Dumitriu, S. Kaliaguine, Mono-and bifunctional MFI, BEA and MCM-41 titanium-molecular sieves. Part 1. Synthesis and characterization, Micropor. Mesopor. Mater. 57 (2003) 169–180.
[41] M.C. Chao, H.P. Lin, C.Y. Mou, B.W. Cheng, C.F. Cheng, Synthesis of nano-sized mesoporous silicas with metal incorporation, Catal. Today 97 (2004) 81–87.
[42] M.V. Cagnoli, S.G. Casuscelli, A.M. Alvarez, J.F. Bengoa, N.G. Gallegos, N.M. Samaniego, M.E. Crivello, G.E. Ghione, C.F. Perez, E.R. Herrero, S.G. Marchetti, "Clean" limonene epoxidation using Ti-MCM-41 catalyst, Appl. Catal. A Gen. 287 (2005) 227–235.
[43] A. Arafat, J.C. Jansen, A.R. Ebaid, H. van Bekkum, Microwave preparation of zeolite Y and ZSM-5, Zeolites 13 (1993) 162–165.
[44] J. Ren, Z. Li, S.S. Liu, Y.L. Xing, K.C. Xie, Silica–titania mixed oxides: Si–O–Ti connectivity, coordination of titanium, and surface acidic properties, Catal. Lett. 124 (2008) 185–194.
[45] G.A. Eimer, S.G. Casuscelli, C.A. Chanquia, V. Elias, M.E. Crivello, E.R. Herrero, The influence of Ti-loading on the acid behavior and on the catalytic efficiency of mesoporous Ti-MCM-41 molecular sieves, Catal. Today 133 (2008) 639–646.
[46] S. Rajagopal, J.A. Marzari, R. Miranda, Silica-alumina-supported Mo oxide catalysts: genesis and demise of Brønsted–Lewis acidity, J. Catal. 151 (1995) 192–203.
[47] M. Sawa, M. Niwa, Y. Murakami, Relationship between acid amount and framework aluminum content in mordenite, Zeolites 10 (1990) 532–538.
[48] F. Lónyi, J. Valyon, On the interpretation of the NH_3–TPD patterns of H-ZSM-5 and H-mordenite, Micropor. Mesopor. Mater. 47 (2001) 293–301.
[49] K.F. Lin, P.P. Pescarmona, H. Vandepitte, D. Liang, G. Van Tendeloo, P.A. Jacobs, Synthesis and catalytic activity of Ti-MCM-41 nanoparticles with highly active titanium sites, J. Catal. 254 (2008) 64–70.
[50] S.P. Wang, X.B. Ma, H.L. Guo, J.L. Gong, X. Yang, G.H. Xu, Characterization and catalytic activity of TiO_2/SiO_2 for transesterification of dimethyl oxalate with phenol, J. Mol. Catal. A Chem. 214 (2004) 273–279.